FEBS Letters 460 (1999) 46–52 FEBS 22742

The X-ray crystal structure of β-ketoacyl [acyl carrier protein] synthase I

Johan Gotthardt Olsen[a,c], Anders Kadziola[a,c], Penny von Wettstein-Knowles[b,*], Mads Siggaard-Andersen[b], Ylva Lindquist[a,c], Sine Larsen[a,c,1]

[a] *Centre for Crystallographic Studies, University of Copenhagen, Universitetsparken 5, DK-2100 Copenhagen, Denmark*
[b] *Department of Genetics, Institute of Molecular Biology, University of Copenhagen, Øster Farimagsgade 2A, DK-1353 Copenhagen, Denmark*
[c] *Division of Structural Biology, Department of Medical Biochemistry and Biophysics, Karolinska Institutet, S-171 77 Stockholm, Sweden*

Received 3 August 1999; received in revised form 20 September 1999

Abstract The crystal structure of the fatty acid elongating enzyme β-ketoacyl [acyl carrier protein] synthase I (KAS I) from *Escherichia coli* has been determined to 2.3 Å resolution by molecular replacement using the recently solved crystal structure of KAS II as a search model. The crystal contains two independent dimers in the asymmetric unit. KAS I assumes the thiolase αβαβα fold. Electrostatic potential distribution reveals an acyl carrier protein docking site and a presumed substrate binding pocket was detected extending the active site. Both subunits contribute to each substrate binding site in the dimer.

Key words: Condensing enzyme; Protein structure; Fatty acid synthesis; *Escherichia coli*

1. Introduction

Each component of the type II fatty acid synthase (FAS) multi-enzyme complexes of bacteria and plant plastids is encoded by a discrete gene, in contrast to the activities of the type I mammalian and yeast type I FASes that are included in one and two multi-functional genes, respectively. The occurrence of isozymes in type II complexes introduces the possibility for synthesizing diverse fatty acyl products. This role is well established for isozymes of β-ketoacyl [acyl carrier protein] synthase (KAS), that is the elongating moiety. Recently more subtle roles of the two dehydratases encoded by *fabA* and *fabZ* have been delineated [1] and a similar role ascribed for the acyl carrier protein (ACP) [2]. In bacteria and plastids three KAS isozymes occur having distinct substrate specificities with respect to chain length, degree of unsaturation and sensitivity to the antibiotic cerulenin [3–5]. KAS III accomplishes the first elongation step from C2 to C4. In plastids KAS I then adds six C2-units to give C16 chains which KAS II can elongate to C18 chains. Bacterial FAS by comparison synthesizes not only saturated fatty acids but also unsaturated fatty acids with the branch point in *Escherichia coli* occurring at 10 carbons. KAS I coded for by *fabB* is a prerequisite for initiation of the unsaturated pathway by elongating *cis* Δ3 C10:1, while KAS II encoded by *fabF* is unique in carrying out the final extension in unsaturated fatty acid synthesis by adding a C2-unit to *cis* Δ9 C16:1 [6–9]. Since the resulting *cis* Δ11 C18:1 fatty acid is not essential and KAS I can replace KAS III by extending C2 to C4 when overexpressed, KAS I is believed to be the only vital β-ketoacyl-ACP synthase in *E. coli* [10]. Interestingly while *E. coli* KAS I and KAS II share 38% identity and 64% similarity [11] *E. coli* KAS II is more closely related to plastid KAS I and KAS II isozymes; for example, *E. coli* and barley KAS II identity is 45% [12,8,13]. This suggests that despite different functions the *E. coli fabF* gene is the progenitor of the plastid genes specifying KAS I and KAS II. KAS III isozymes not only have limited homology to KAS I and KAS II [14,15], but also use a coenzyme A activated primer substrate rather than an ACP activated one [16,17].

The Claisen condensation catalyzed by KAS I and KAS II is tripartite: (1) transthioesterification of the fatty acyl primer substrate from the pantotheine arm of ACP to the enzyme, (2) decarboxylation of the donor malonyl-ACP substrate to give an acetyl-ACP carbanion and (3) nucleophilic attack of the carbanion on the carbon atom of the thioester to form the elongated β-ketoacyl-ACP product. At least three residues participate directly in catalysis. The active site, substrate binding cysteine, Cys-163, of *E. coli* KAS I was identified a number of years ago [11], and recently the two histidines, His-298 and His-333, predicted to act in catalysis [14], have been shown to do so by in vitro mutagenesis and enzymatic analyses of overexpressed wild-type and mutant proteins [18]. In accord with these observations, the β-ketoacyl-ACP synthase inhibitor, cerulenin, has been complexed with the analogous cysteine in crystals of *E. coli* KAS II [19] in which the analogous His residues are close enough to the active site cysteine to participate in catalysis [20]. In the present paper we present the crystal structure of the essential *E. coli* KAS I isozyme to 2.3 Å resolution and make a comparison with the KAS II crystal structure.

2. Materials and methods

2.1. Protein preparation and crystallization

A recombinant KAS I from *E. coli* with the N-terminally His-tagged sequence (MetArgGlySerHisHisHisHisHisHisGlySer) was expressed and purified as described [18], except that an additional purification step was necessary. The major peak eluting from the Ni-NTA column was dialyzed against 50 mM Tris, 2 mM ethylenediamine tetra-acetate disodium salt and 1 mM dithiotreitol (buffer A) and loaded onto an anion exchange column (monoQ 5/5, 1 ml column bed volume) at approximately 15 mg protein per ml bed volume. The protein was eluted in a linear 0–1 M NaCl gradient in 100 ml buffer A.

Crystallization was performed as described previously [21]. Crystals

*Corresponding author. Fax: (45) 35322110.
E-mail: knowles@biobase.dk

[1] Also corresponding author. Fax: (46) (8) 327626;
E-mail: sine@xray.ki.ku.dk

Abbreviations: KAS, β-ketoacyl [acyl carrier protein] synthase; FAS, fatty acid synthase; ACP, acyl carrier protein; NCS, non-crystallographic symmetry; PKS, polyketide synthase

PII: S0014-5793(99)01303-4

of the recombinant His-tag extended protein were obtained under the same conditions as for the wild-type enzyme. They belong to the same space group, $P2_12_12_1$ and have the same cell dimensions, $a = 59.62$ $b = 142.71$ $c = 213.46$ [21].

2.2. Data collection

X-ray data were recorded from a single crystal at 18°C with an R-AXIS II imaging-plate system employing graphite monochromatized CuKα radiation produced with a Rigaku Rotaflex RU 200 rotating anode operating at 50 kV and 180 mA. 200 non-overlapping images were collected, each covering a 0.5° oscillation range with a crystal to detector distance of 120 mm. The images were exposed for 30 min each. Integrated intensities were obtained and reduced with HKL suite programs DENZO and SCALEPACK, respectively [22].

The data reduction resulted in a 94.3% complete data set (51.0% for the outer resolution shell, 2.34–2.30 Å) comprising 76863 unique reflections in the resolution range 30.0–2.30 Å. R_{merge} was 7.8% (13.0% for the outer shell) with an average redundancy of 3.0 and an overall $\langle I/\sigma I\rangle$ of 10.6 (4.1 for the outer shell). Data collection statistics are summarized in Table 1.

2.3. Structure determination

The KAS I structure was solved by molecular replacement (MR) using the KAS II crystal structure [20] as a search model. The two proteins share 38% sequence identity [8], and the search model was not trimmed in any way. The structure could be solved by placing four monomers or two dimers in the asymmetric unit. We used the automated script version of the MR program AMoRe [23] with the 'centered correlation function' (CC option) for all translational searches [24]. Reflections in the resolution range 15.0–3.5 Å were used for all MR calculations. For the monomer search, what proved to be the four correct solutions were ranked # 1, # 2, # 3 and # 8 in the fast rotation function. After the translational search placing the first monomer, these rotation solutions moved to the top regarding all criteria (highest correlation coefficients on F's and I's and lowest R-factors), however, with a poor contrast. At this stage, the best correlation on F's and the lowest R-factor was 11.1% and 54.2%, respectively. Positioning of the monomers in turn led to the following increasing sequence of F correlations: 11.1%, 17.3%, 22.4%, 28.3% paralleled by decreasing R-factors: 54.2%, 52.6%, 51.3%, 49.5%. Independent rigid body refinement of the four subunits in the asymmetric unit improved the F correlation and the R-factor to 32.4% and 48.1%, respectively, and now with a clear contrast.

When space group symmetry was applied to the MR solution, no overlaps were detected in the crystal packing. The four molecules are arranged as two dimers in the asymmetric unit, consistent with the dimer found in the KAS II structure. From the MR solution NCS-averaged 2 mF_o–DF_c and mF_o–DF_c maps [25–27] were produced using only backbone atom (C_α, N, O, C) contributions to F_c. In these maps, side chain densities which could be interpreted in terms of the KAS I sequence were visible for the major part of the structure, indicating a successful structure determination.

2.4. Refinement

The KAS I structure was refined with X-PLOR [28] using the Engh and Huber structural parameter set [29]. A 5% test data set was selected at random for R-free evaluation [30]. We used NCS-restraints throughout all refinement steps. Between refinements, the model was manually reconstructed from the four-fold NCS-averaged 2 mF_o–DF_c and mF_o–DF_c maps [25–27]. This was done using the graphics display program TURBO-FRODO [31]. The initial map was based on backbone atoms from the rigid body refined MR solution. This cautious approach was followed at each reconstruction round. Structural parts which were not clear from the density maps were omitted from the subsequent refinement and map calculation. Until the entire KAS I sequence was correctly assigned, only one overall B-factor was refined. Refinement with four copies of the complete sequence (residues 1–406) with overall B-factor refinement gave an R_{work} of 26.2% and an R_{free} of 28.0%. Subsequent neighbor- and NCS-restrained B-factor optimization reduced those values to 20.7% and 22.9%, respectively.

The electron densities in the resulting NCS-averaged 2 mF_o–DF_c and mF_o–DF_c maps showed clear evidence of water molecules. To avoid overparametrization, we decided to include only NCS-related water molecules which appear in all four monomers and which therefore may be considered structural. Water molecules which appeared in the averaged maps with sensible hydrogen bonding geometry were included in the refinement and kept in the model, if they refined with B-factors below 55 Å^2 and were well defined in the map.

The KAS I model consists of four NCS related molecules with structural water: 406 amino acid residues and 127 water molecules per subunit. This model has been refined with data between 10.0 and 2.3 resolution giving an R-factor of 18.8% (71920 reflections) and an R-free of 21.9% (3809 reflections, 5% of total). The electron density i.e. the NCS-averaged 2 mF_o–DF_c map is well resolved for all residues except for the termini and some side chains involved in crystal packing, where some disorder is seen. The model displays good stereo chemistry with R.M.S. deviations from tabulated values of 0.013 for bond distances and 1.540° for angles. A Ramachandran plot calculated with PROCHECK [32] revealed 91.3%, 6.7% and 1.7% of the non-glycine/proline residues in the most favored, additionally allowed and generously allowed regions, respectively. One residue in each subunit, Leu-335, is found in the disallowed region with (ϕ,ψ)-angles of (52°, 110°). This residue has a well resolved electron density and is situated in the active site near Cys-163.

3. Results and discussion

3.1. Overall structure

Sedimentation and gel filtration experiments have shown that KAS I and II are dimeric enzymes in solution [6,7,33]. The crystal structure of KAS I contains four independent, but virtually identical subunits in the asymmetric unit. These pair around two two-fold axes to form two dimers. In contrast, KAS II crystallizes with only one molecule in the asymmetric unit and the dimer two-fold axis coincides with a crystallographic two-fold.

KAS I adopts the thiolase fold, first described for yeast peroxisomal thiolase [34,35]. The 406 amino acid polypeptide folds into two α-β-α domains sandwiched together to form an α-β-α-β-α 'double whopper' structure (Fig. 2). Both β-sheets are mixed with connectivity $+3x$, $+1x$, $-2x$, -1, using the nomenclature devised by Richardson [36]. The nomenclature of the thiolase secondary structure elements was employed for KAS I (Fig. 2). Secondary structure was assigned in TURBO-FRODO [31] based on the principles by Kabsch and Sander [37]. A central five stranded anti-parallel β-sheet surrounded

Table 1
Data collection, refinement and B-factor statistics

Data collection statistics (30–2.3 Å)	
Unique Reflections	76863
R_{merge} (%)	7.8 (13.0)
Completeness (%)	94.3 (51.0)[a]
$\langle I/\sigma I\rangle$	10.6 (4.1)[a]
Refinement statistics (10–2.3 Å)	
Unique reflections	75729
R_{work} (%)	18.8 (25.1)[b]
R_{free} (%)	21.9 (29.2)[b]
R.M.S. deviation from ideal bond lengths (Å)	0.013
R.M.S. deviation from ideal bond angles (°)	1.54°
Atomic B-factor statistics (Å^2)	
$\langle B\rangle$ protein	14.6
$\langle B\rangle$ main chain atoms	12.9
$\langle B\rangle$ side chain atoms	15.2
$\langle B\rangle$ solvent	24.8
$\langle B\rangle$ total	15.0

[a]Values for outer resolution shell (2.34–2.3 Å);
[b]Values for outer resolution shell (2.4–2.3 Å). The internal R-value, $R_{merge} = \Sigma_{hkl,i}|I_{hkl,i} - \langle I\rangle_{hkl}|/\Sigma_{hkl,i}I_{hkl,i}$, where $I_{hkl,i} = i$th observed intensity of the unique reflection hkl and $\langle I\rangle_{hkl}$ = average intensity obtained from multiple observations of symmetry related reflections. R_{work} and R_{free} are the R-values for 95% of the reflections used in refinement and 5% not used in refinement but for cross validation. The R-values are defined as $R = \Sigma||F_o| - |F_c||/\Sigma|F_o|$.

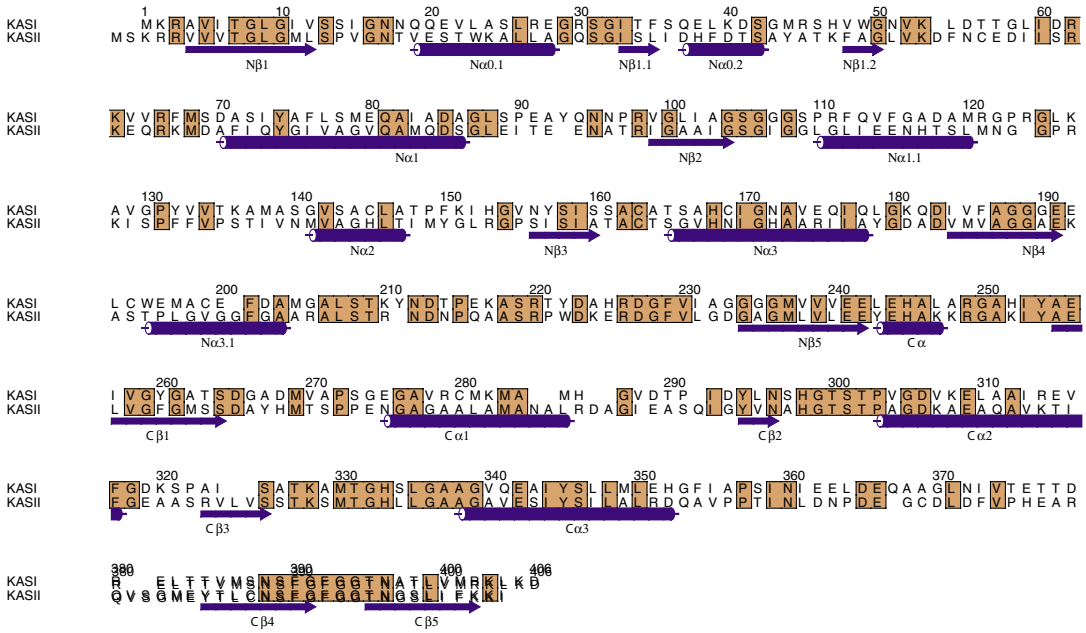

Fig. 1. Alignment of the amino acid sequences of KAS I and KAS II. The position of secondary structural elements as calculated for KAS I are shown below with assigned labels. Residues that are conserved between the two sequences are emphasized with red boxes.

by α-helices defines both domains in the thiolase fold. The three structures, KAS I, KAS II and thiolase have six α-helices in common that are equally distributed between the two domains, three in each. Another feature common for the three structures is the interaction between the subunits through the short Nβ3 strands related by two-fold symmetry. The hydrogen bonds between the backbone atoms connect the β-strands in the N-terminal domains to form a continuous 10 stranded β-sheet traversing the entire length of the dimer, displaying a right handed twist of 156° for KAS I. The Cβ-sheets cap the central sheet creating a tunnel harboring the Cα3 and Nα3 helices. These helices assume the shape of an M in the dimer (Fig. 3).

In addition to its core domain, thiolase has a long loop 'on top' of the molecule (as seen in the same orientation as in Fig. 3). In KAS I and II the latter is replaced by a capping domain. In KAS I, the cap of this domain, consisting of Nβ1.1 and Nβ1.2 along with Nα0.2 and Nα3.1, effectively seals the active site from this approach. The visor of the cap, situated towards the interface, is defined by Nα1.1, a long loop, and

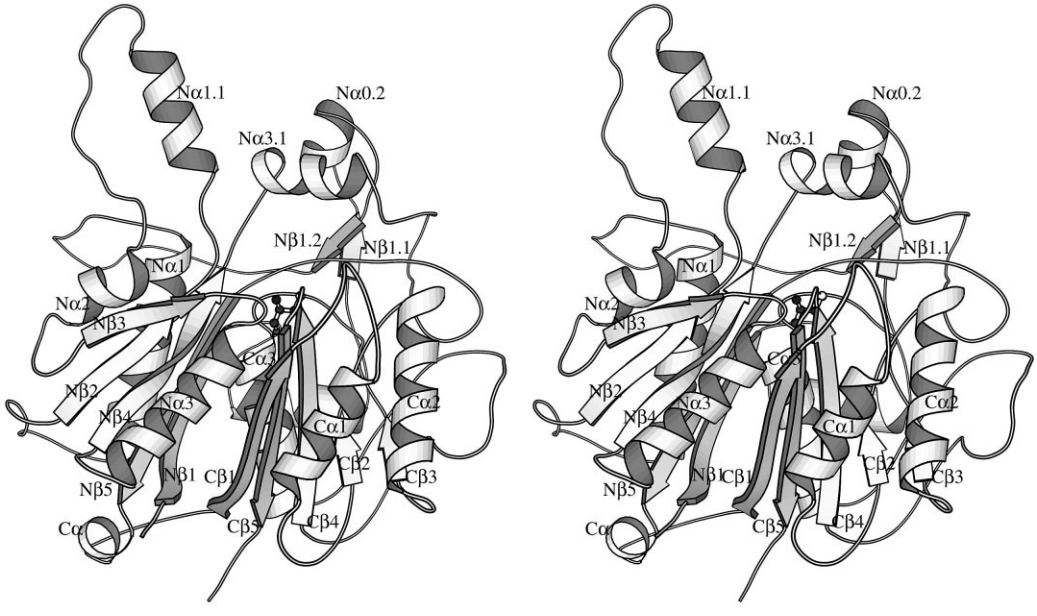

Fig. 2. A schematic outline of the fold of the KAS I subunit. Active site Cys-163 shown in ball-and-stick representation. Following the nomenclature proposed by Mathieu et al. for the thiolase fold [34], the N-terminal β-sheet is called Nβ and the individual strands are denoted Nβ1, Nβ2, etc. An α-helix outside the thiolase core situated immediately after core helix Nα1 is called Nα1.1. The secondary structure assignment was performed automatically using the Karbsch-Sander algorithm [37]. The figure was constructed with the program Molscript [42].

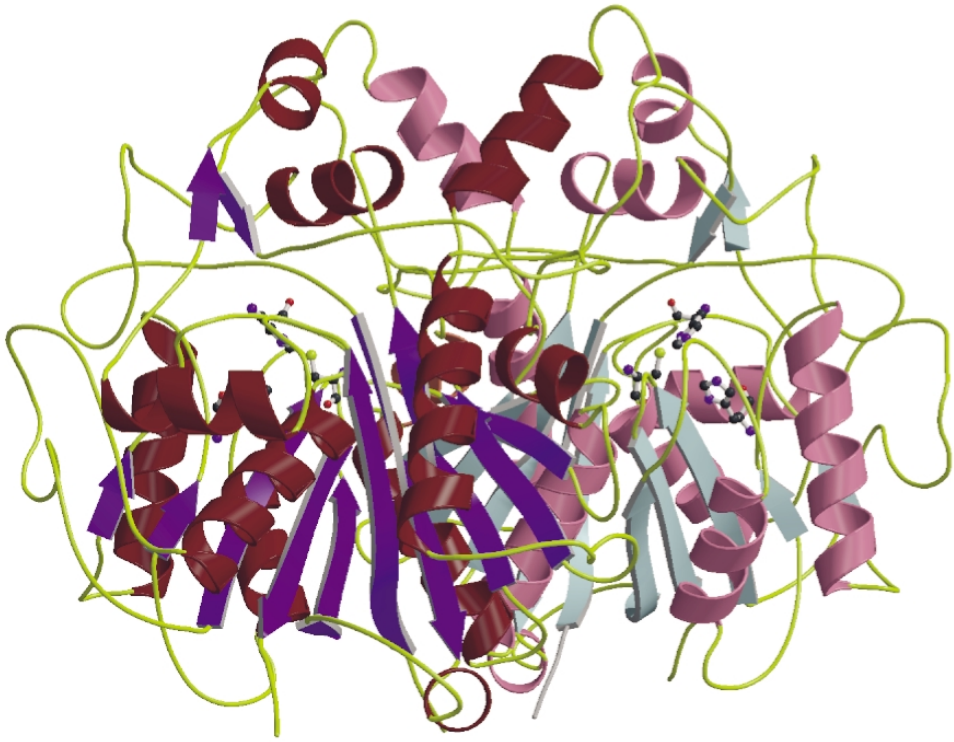

Fig. 3. Ribbon structure of the KAS I dimer as viewed perpendicular to the two-fold axis. Helices and strands are red and blue respectively in the subunit on the right and pink and light blue in the subunit on the left. Active site residues Cys-163, His-298, and His-333 are shown in ball and stick representation. The site on the right is accessible from above the page, the other from below. Notice the well-defined separation of secondary structural elements from the capping domain on top and the thiolase core domain below. Constructed using Molscript [42].

Nα2. The latter two α-helices from both subunits interact to form an extra dimer interface region extending upward from the core interface.

3.2. Comparison with KAS II

KAS I and KAS II share 38% sequence identity (Fig. 1). Not surprisingly they exhibit very similar folds which proved useful in determining the structure of KAS I. An inspection of Fig. 1 reveals that the conserved residues are more concentrated in the C-than in the N-terminal domain. This is also reflected in the results from the structural alignments of the two structures. Superposition of Cα atoms of the C-terminal domains from the two structures results in an r.m.s. for the Cα atoms of 0.65 Å, whereas the equivalent superposition of the N-terminal domains gives a significantly higher R.M.S. of 0.95 Å. Superposition of the Cα atoms of the entire structures yields an R.M.S. of 0.85 Å Apart from small variations in the length of the common α-helices and β-strands, the KAS II structure contains two additional short β-strands in the long loop region that connects Cα3 and Cβ4 in the KAS I structure. Small α-helices have also been assigned in KAS II in the stretches of highly conserved residues encompassing amino acids 220 and 330 (Fig. 1). The α-helix αN0.2 in KAS I lacks a match in the KAS II structure which instead has an additional α-helix between Nα1.1 and Nα2. Since all these additional structural elements cover very short stretches of three to six residues in the polypeptide chain, they do not perturb the general picture of KAS I and KAS II sharing the same fold.

Each KAS I subunit donates 2348 $Å^2$ or 17.8% of the surface area to the dimer interface. In addition the hydrogen bond interactions between the two Nβ5 strands and the two salt bridges, Arg-121–Asp118 plus Lys-181–Glu-175, tie the two subunits together. Though this interface contains a few other hydrogen bonds, hydrophobic interactions seem to play an equally important role. In spite of the fact that none of the residues involved in the interactions in this dimer are conserved between KAS I and KAS II, we found it worthwhile to evaluate the possibility of formation of a hetero dimer composed of KAS I and II subunits. In *Streptomyces coelicolor* polyketide synthases (PKS's) exist producing aromatic antibiotics whose KAS counterparts are also dimeric. In contrast to *E. coli* KAS enzymes, the PKS enzymes are heterodimers built up from one subunit lacking an active site cysteine and one with this residue [38]. The catalytically inactive subunit is essential for enzymatic function and has been implicated in chain length determination. A hypothetical heterodimer was constructed from the structures of KAS I and KAS II and close examination of the interface interactions did not reveal structural features that would rule out hetero-dimer formation. The few clashes observed could readily be avoided by rearrangements of the pertinent side chains. The potential for hydrogen bonding and hydrophobic interactions is comparable to that found in the homodimers.

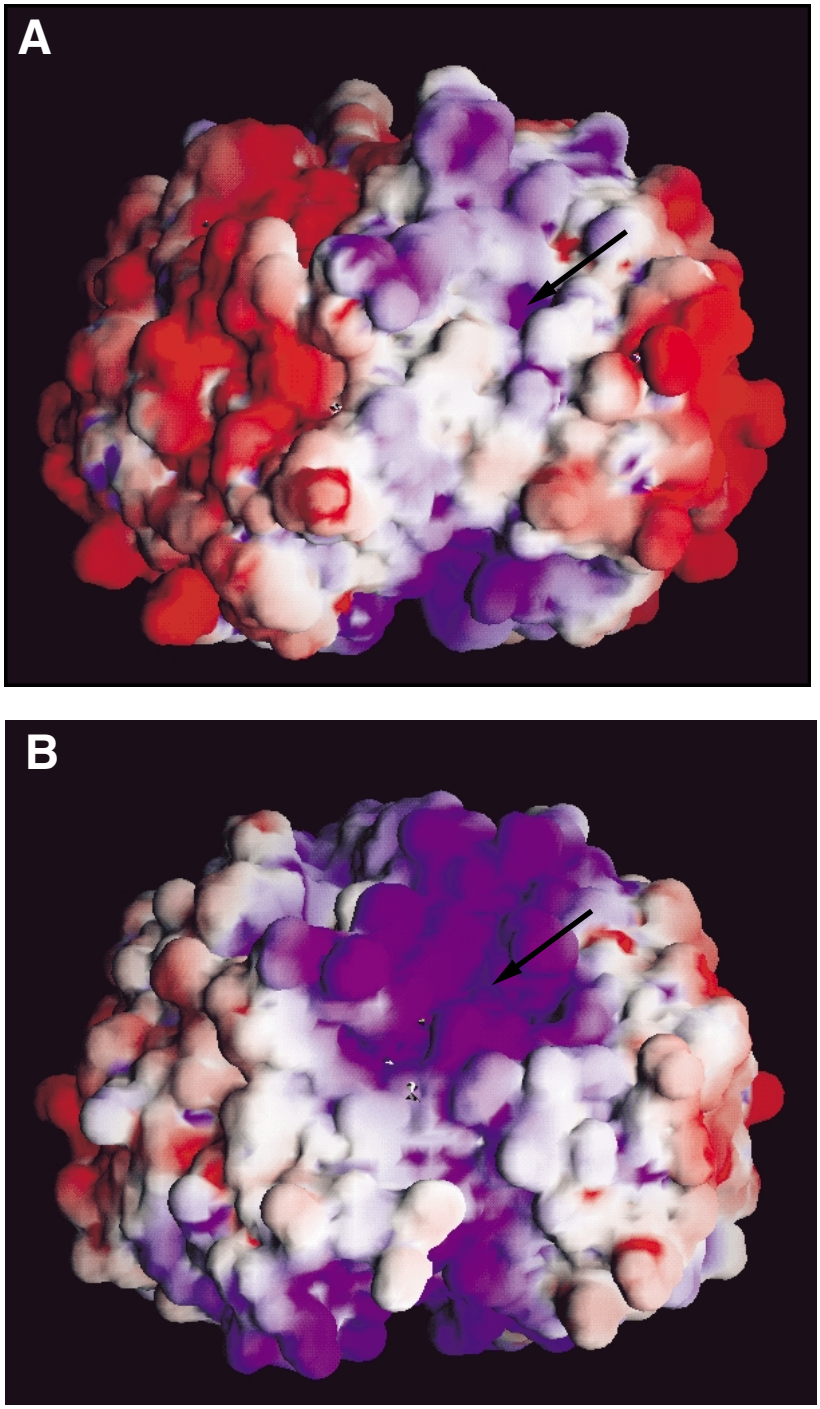

Fig. 4. A and B: Accessible surface map representation of electrostatic potential distribution on the KAS I and KAS II dimer, respectively. Orientation is the same as in Fig. 3. Positive and negative electrostatic potentials are colored blue and red, respectively. Notice that the overall distribution of charges is the same: Positive potential around the active site flanked by strong negative potential. An arrow points to the active site entrances.

Mapping the electrostatic potential [39] on the two dimers reveals that both surfaces are predominantly negative except for a strip of positive potential extending from one active site to the other (Fig. 4A and B). The acyl carrying polypeptide, ACP has an abundance of negatively charged side chains. The apparent surface charge distribution is consistent with an ACP docking functionality around the active site. The same pattern of calculated charge distribution occurs on the ACP interacting *E. coli* FAS enzymes enoyl reductase [40] and malonyl-CoA:ACP transacylase [41], namely positive around the active site, negative potential dominating the rest of the enzyme surface.

3.3. The active site

The centerpiece of the active site is the cysteine residue, Cys-163, which accepts the acyl chain from the substrate donor, acyl-ACP via a thioester. Two almost perpendicular histidine side chains point towards the cysteine. One of these,

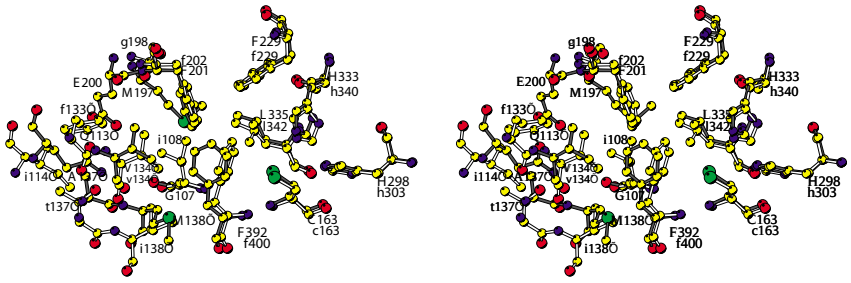

Fig. 5. Superposition of the active sites and presumed binding pockets of KAS I (dark gray sticks) and KAS II (white sticks) in ball-and-stick representation. KAS I residues are labelled with capital letters and KAS II residues in lower case, those marked with ' are from the other subunit in the dimer. The Cα of KAS II Ile-108 overlaps with the Cα of KAS I Gly-107, and its side chain points into the cavity in KAS I. The KAS II structural equivalent to KAS I Met-197 is Gly-198. The KAS II equivalent to Gln-113' is Ile-114' and the space occupied by Glu-200 is partially filled by Phe-133'. Glu-200 and Gln-113' are at the bottom of the KAS I cavity. The only polar residue in the KAS II binding pocket is Thr-137' which is an alanine in KAS I.

His-333 makes a hydrogen bond to Cys-163 Sγ, while the other, His-298 connects to Cys-163 Sγ via a water molecule. These residues are completely conserved among decarboxylating condensing enzymes [14] and have been shown to participate in catalysis [18].

The active sites in the KAS I dimer are accessible at the bottom of narrow funnels defined by Phe-201, Phe-229, Phe-390, Phe-392 and Thr-300. The spatial equivalent to the thiolase active site access area is covered completely by the cap of the capping domain defined by secondary structure elements Nα0.2, Nβ1.1, Nβ1.2, Nα1.1, and Nα3.1 as described in Section 3.1 and (Fig. 2).

In each KAS I subunit a 163 Å^3 cavity stretches from the active site cysteine 163 to glutamine 113, located on the other subunit (Fig. 5). The distance between the two specified side chains is circa 16 Å which seems reasonable for harboring the KAS I substrates. The two Gln-113s, which are located on the interface of the visor cap, are linked by hydrogen bonds. Residues Gly-107, Met-197, Glu-200, Phe-201, Leu-335, Phe-392 plus Val-134 and Met-138 coming from the other subunit line the cavity with the side chain of Glu-200 pointing inward. Similar calculations do not reveal this cavity in the uncomplexed KAS II structure. Recently, the crystal structure of KAS II in complex with the inhibitor cerulenin was determined to 2.65 Å resolution [19] revealing the inhibitor where we see the cavity in KAS I. In the uncomplexed KAS II structure [20] this cavity was occluded by the side chains of Phe-400 (Phe-392 in KAS I) and Ile-108 which thus have to change rotamer conformation to accommodate substrates of corresponding length (Fig. 5). This is in contrast to uncomplexed KAS I where the cavity is open and Phe-392 has a conformation that facilitates access to the binding pocket. Furthermore Ile-108 is replaced by a glycine in KAS I.

The comparison of the cavity structures reveals the probable basis for the differences in substrate specificities between KAS I and KAS II; KAS II is able to harbor a two carbon atoms longer substrate and with a *cis* double bond at position 9. The isoleucine to glycine substitution mentioned above combined with the substitution of Gly-198 to Met-197 in KAS I changes the outline of the cavity without really affecting its size. KAS I in contrast to KAS II is able to elongate *cis* Δ3 C10:1 and KAS II is essential for the elongation of *cis* Δ9 C16:1 to *cis* Δ11 C18:1. The double bond changes position relative to the carboxyl moiety of the substrate. The nature of the binding pocket in KAS II must be so that it prevents binding of the initial unsaturated substrate (*cis* Δ3 C10:1). This may indicate that the short chain unsaturated acyl chain is hindered access to KAS II because of the shape of the binding pocket whereas C18:1 is incompatible with KAS I primarily because the binding pocket in this case is simply not deep enough.

From the structure of the cerulenin-KAS II complex it was postulated that further structural adjustments have to take place to bind the longest substrates and some rotation of Phe-133, at the end of the cavity, was suggested as likely. This residue is a valine in KAS I and in the region occupied by the phenylalanine side chain in KAS II, KAS I has the charged side chain of Glu-200 (Gly-201 in KAS II). This side chain would come too close for long substrates and charge repulsion should thus prevent access of a hydrophobic substrate to its vicinity at the end of the channel.

3.4. Conclusions

We conclude that (1) the overall structures of KAS I and II are highly similar with respect to folding topology and surface electrostatic potential. (2) Electrostatic potential mapping of KAS I and II as well as other ACP binding enzymes of the *E. coli* FAS reveals a pattern which may well be general to these enzymes. An overall negative potential except for a strong positive potential encompassing and, in the case of oligomeric enzymes connecting the active sites. This pattern seems ideal for specific docking of the negatively charged ACP molecule. (3) KAS I has a cavity which is very similar to the cerulenin binding pocket seen in the KAS II-cerulenin complex structure [19]. This cavity is less hydrophobic in character than the KAS II cavity, indeed a negatively charged residue at one end of the cavity probably limits the substrate carbon chain length. Furthermore, differences in the form of the cavity can explain discrimination among the *cis* unsaturated fatty acid substrates. In contrast to KAS II, contact between the two substrate binding cavities in the KAS I dimer seems hindered by residues on the interface. This observation has implications for differences in substrate specificity.

References

[1] Heath, R.J. and Rock, C.O. (1996) J. Biol. Chem. 271 (44), 27795–27801.
[2] Suh, M.C., Schultz, D.J. and Ohlrogge, J.B. (1999) Plant J. 17, 679–688.

[3] Magnuson, K., Jackowski, S., Rock, C.O. and Cronan, J.E. (1993) Microbiol. Rev. 57, 522–542.
[4] Harwood, J.L. (1996) Biochim. Biophys. Acta, 1301, 7–56.
[5] Siggaard-Andersen, M. (1988) Carlsberg Res. Commun. 53, 371–379.
[6] D'Agnolo, G., Rosenfeld, I.S. and Vagelos, P.R. (1975) J. Biol. Chem. 250 (14), 5289–5294.
[7] Garwin, J.L., Klages, A.L. and Cronan, J.E. (1980) J. Biol. Chem. 255 (24), 11949–11956.
[8] Siggaard-Andersen, M., Wissenbach, M., Chuck, J.-A., Svendsen, I., Olsen, J.G. and von Wettstein-Knowles, P. (1994) Proc. Natl. Acad. Sci. USA 91, 11027–11031.
[9] Magnuson, K., Carey, M.R. and Cronan, J.E. (1995) J. Bacteriol. 177, 3593–3595.
[10] Tsay, J.-T., Rock, C.O. and Jackowski, S. (1992) J. Bacteriol. 174, 508–513.
[11] Kauppinen, S., Siggaard-Andersen, M. and von Wettstein-Knowles, P. (1988) Carlsberg Res. Commun. 53, 357–370.
[12] Siggaard-Andersen, M., Kauppinen, S. and Wettstein-Knowles, P.v. (1991) Proc. Natl. Acad. Sci. USA 88, 4114–4118.
[13] Wissenbach, M. (1994) Plant Physiol. 106, 1711–1712.
[14] Siggaard-Andersen, M. (1993) Protein Seq. Data Anal. 5, 325–335.
[15] Tai, H. and Jaworski, J.G. (1993) Plant Physiol. 103, 1361–1367.
[16] Tsay, J.-T., Oh, W., Larson, T.J., Jackowski, S. and Rock, C.O. (1992) J. Biol. Chem. 267, 6807–6814.
[17] Clough, R.C., Matthis, A.L., Barnum, S.R. and Jaworski, J.G. (1992) J. Biol. Chem. 267, 20992–20998.
[18] Siggaard-Andersen, M., Bangera, G., Olsen, J.G., and von Wettstein-Knowles, P. (1998) in: Advances in Plant Lipid Research (Sánchez, J., Cerdá Olmedo, E., and Martínez-Force, E., Eds), pp. 67–70, Universidad de Sevilla. Secretariado de Publicaciones.
[19] Moche, A., Schneider, G., Edwards, P., Dehesh, K. and Lindqvist, Y. (1999) J. Biol. Chem. 274, 6031–6034.
[20] Huang, W., Jia, J., Edwards, P., Dehesh, K., Schneider, G. and Lindqvist, Y. (1998) EMBO J. 17, 1183–1191.
[21] Olsen, J.G., Kadziola, A., Siggaard-Andersen, M., Chuck, J.-A., Larsen, S. and von Wettstein-Knowles, P. (1995) Protein Pept. Lett. 1, 246–251.
[22] Otwinowski, Z. and Minor, W. (1997) Methods Enzymol. 276, 307–326.
[23] Navaza, J. (1994) Acta Crystallogr. Sect. A 50, 157–163.
[24] Navaza, J. and Vernoslova, E. (1995) Acta Crystallogr. Sect. A 51, 445–449.
[25] Computational Project number 4, C., (1991) Acta Crystallogr. Sect. D 50, 760–763.
[26] Read, R. (1986) Acta Crystallogr. Sect. A 42, 140–149.
[27] Kleywegt, G.J. and Read, R.J. (1997) Structure 5, 1557–1569.
[28] Brünger, A. X-PLOR Version 3.1: a System for X-ray Crystallography and NMR, Yale University Press, New Haven, CT.
[29] Engh, R.A. and Huber, R. (1991) Acta Crystallogr. Sect. A 47, 392–400.
[30] Brünger, A. (1992) Nature 355, 472–475.
[31] Roussel, A. and Cambillau, C. (1992) Architecture et Fonction des Macromolécules Biologiques, TURBO-FRODO, Biographics and AFMB, Marseille.
[32] Laskowski, R.A., MacArthur, M.V., Moss, D.S. and Thornton, J.M. (1993) J. Appl. Crystallogr. 26, 283–291.
[33] Edwards, P., Nelsen, J.S., Metz, J.G. and Dehesh, K. (1997) FEBS Lett. 402, 62–66.
[34] Mathieu, M., Zeelen, J.P., Erdmann, R., Kunau, W.-H. and Wierenga, R.K. (1994) Structure 2, 797–808.
[35] Mathieu, M., Modis, Y., Zeelen, J.P., Engel, C.K., Abagyan, R.A., Ahlberg, A., Rasmussen, B., Lamzin, V., Kunau, W.H. and Wierenga, R.K. (1997) J. Mol. Biol. 273, 714–728.
[36] Richardson, J.S. (1981) Adv. Protein Chem. 34, 167–339.
[37] Kabsch, W. and Sander, C. (1983) Biopolymers 22, 2577–2637.
[38] Sherman, D.H., Eung-Soo, K., Bibb, M.J. and Hopwood, D.A. (1992) J. Bacteriol. 174, 6184–6190.
[39] Nicholls, A., Sharp, K.A. and Honig, B. (1991) Proteins 11, 281–296.
[40] Baldcock, C., Rafferty, J.B., Sedelnikova, S.E., Baker, P.J., Stuitje, A.R., Slabas, A.R., Hawkes, T.R. and Rice, D.W. (1996) Science 274, 2107–2110.
[41] Serre, L., Verbree, E.C., Dauter, Z., Stuitje, A.R. and Derewenda, Z.S. (1995) J. Biol. Chem. 270, 12961–12964.
[42] Kraulis, P. (1991) J. Appl. Crystallogr. 24, 946–950.